Phonon Transport in Isotope-Disordered Carbon and Boron-Nitride Nanotubes: Is Localization Observable?

Ivana Savić,[1] Natalio Mingo,[1,2] and Derek A. Stewart[3]
[1]*LITEN, CEA-Grenoble, 17 rue des Martyrs, 38054 Grenoble Cedex 9, France*
[2]*UC Santa Cruz, Santa Cruz, California 95064, USA*
[3]*Cornell Nanoscale Facility, Cornell University, Ithaca, New York 14853, USA*
(Received 22 May 2008; published 13 October 2008)

We present an *ab initio* study which identifies dominant effects leading to thermal conductivity reductions in carbon and boron-nitride nanotubes with isotope disorder. Our analysis reveals that, contrary to previous speculations, localization effects cannot be observed in the thermal conductivity measurements. Observable reduction of the thermal conductivity is mostly due to diffusive scattering. Multiple scattering induced interference effects were found to be prominent for isotope concentrations $\gtrsim 10\%$; otherwise, the thermal conduction is mainly determined by independent scattering contributions of single isotopes. We give explicit predictions of the effect of isotope disorder on nanotube thermal conductivity that can be directly compared with experiments.

DOI: 10.1103/PhysRevLett.101.165502 PACS numbers: 63.22.−m, 65.80.+n, 66.70.−f, 68.65.−k

In recent years, it has become possible to experimentally study the flow of heat at the nanoscale [1]. This has opened up a new field, with plenty of novel phenomena which are not yet understood. One specific issue that is still controversial is the effect of isotope disorder on nanotube thermal conduction, which has been experimentally investigated in boron-nitride (BN) nanotubes (NTs) [2]. Despite the fact that thermal transport in disordered quasi-one-dimensional (1D) systems has been addressed in several theoretical studies [3–14], a detailed analysis of this problem in realistic systems at the atomic scale is still lacking. Previous work has focused on short nanowires (NWs) and thin films with rough surface [3–8] and isotope impurities [9]. Also, carbon NTs (CNTs) in the presence of structural or chemical defects [10–12] and isotope impurities [13,14] have been investigated. Although these studies proved to be useful in estimating a reduction of the thermal conductance with respect to the defect free case, its deviation from the universal value at low temperatures [6], and its anomalous temperature behavior in thin NWs [7], they have only touched upon the important issue of coherent transport regimes and their implications on thermal conduction.

It is well known from transport theory that wave interference (WI) effects in disordered systems lead to distinct transport regimes: ballistic, diffusive and localized [15]. It has been speculated that localized phonon transport might be the reason for a large reduction (50%) of the thermal conductivity in isotope-disordered BN NTs [2]. However, to our best knowledge, no study has attempted to calculate characteristic transport length scales, and answer whether or not this is the case. In this Letter, we resolve the existing controversy and show that localization effects should not be observable. Instead, diffusive scattering is the dominant mechanism which decreases the thermal conductivity. The contribution of multiple scattering driven WI effects to thermal conduction is considerable for large isotope concentrations ($\gtrsim 10\%$); for low concentrations, scattering properties of individual isotope impurities play a dominant role. We present these findings for C and BN NTs with isotope disorder and give concrete predictions of the magnitude of isotope effects on their thermal conductivities.

The issue of phonon transport in disordered quasi-1D systems is conceptually similar to that of electron transport [16,17]. We use an atomistic Green's function formalism [18] to study coherent phonon transport in nanotubes with isotope disorder. *Ab initio* interatomic force constants of perfect infinite C and BN NTs were calculated with an atomic orbital pseudopotential density functional approach [19] using converged parameters given in previous works [12,20]. Introducing isotopes modifies the harmonic matrices via the altered masses only, without changing the force constants. We consider a nanotube segment of length L, containing a random configuration of isotopes and connected to perfect, semi-infinite leads [see Fig. 1(a)]. Assuming an infinitely small temperature gradient between the leads, the transmission function through the disordered section of different lengths (up to 5 μm), for the whole frequency spectrum, is calculated [18,21]. The same procedure is repeated for a sufficient number of different random configurations (200) of isotope impurities in the same concentration, and the configuration averaged transmission for each frequency and length is computed. Finally, the thermal conductance σ is calculated according to $\sigma = \int_0^\infty \frac{\hbar\omega}{2\pi} \overline{\mathcal{T}}(\omega) \frac{df_{\mathrm{BE}}(\omega,T)}{dT} d\omega$, where $\hbar$ is Planck's constant, ω the phonon angular frequency, T the temperature, $\overline{\mathcal{T}}(\omega)$ the configuration averaged transmission, and $f_{\mathrm{BE}}(\omega, T)$ the Bose-Einstein distribution.

Figure 1(b) shows how the configuration averaged transmission depends on the frequency for different lengths L of a (7, 0) CNT with 10.7% of ^{14}C isotope impurities. The transmission of the perfect nanotube (solid black line) matches the number of phonon bands N. The transmission for low frequencies weakly varies with the length. This is a

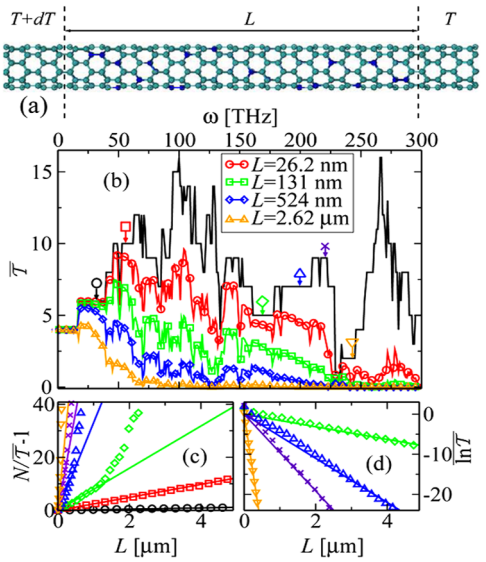

FIG. 1 (color online). (a) Illustration of a nanotube section of length L which contains a random configuration of isotopes (shown in dark color) and is connected to perfect, semi-infinite leads kept at an infinitesimal temperature difference dT. (b) Transmission averaged over 200 random configurations of disorder ($\overline{\mathcal{T}}$) versus frequency dependence for several lengths of (7, 0) carbon nanotubes with 10.7% of ^{14}C isotopes. The solid black line corresponds to the perfect nanotube case. (c) $N/\overline{\mathcal{T}} - 1$, where N is the number of phonon bands of the perfect nanotube, as a function of the length for the frequencies indicated by arrows in (a). Solid lines correspond to linear fits which give mean free paths. (d) Configuration averaged logarithm of transmission ($\ln\overline{\mathcal{T}}$) as a function of the length for the frequencies indicated by arrows in (a). Solid lines correspond to linear fits which give localization lengths.

characteristic of the ballistic transport regime. For higher frequencies, multiple scattering events start dominating the transport as L increases and a crossover from the ballistic to the diffusive regime occurs. This is clearly seen in Fig. 1(c): the length dependence of the transmission for intermediate frequencies (except those close to the band edges), given by circles and squares in Fig. 1(b), is well described by the sum of the ballistic and diffusive contributions in the entire range of L considered: $\overline{\mathcal{T}}(\omega) = N/(1 + L/l_e(\omega))$, where $l_e(\omega)$ is the mean free path [15]. However, for high frequencies and those close to the band edges, isotope induced backscattering effects become increasingly important as L increases. As a consequence, the localization regime is established, characterized by an exponential decrease of the transmission with the length according to $\ln\overline{\mathcal{T}}(\omega) = -L/\xi(\omega)$, where $\xi(\omega)$ is the localization length [15]. In Fig. 1(c), the transmission at frequencies indicated by diamonds, triangles, crosses, and upper triangles in Fig. 1(b) clearly fits the dif fusive scaling law for small L. For larger L, the transmission is well represented by the localization scaling law [see Fig. 1(d)].

To fully characterize coherent transport regimes, we have calculated the frequency dependence of the mean free paths and the localization lengths (given in Fig. 2 by solid and dashed lines, respectively). The mean free paths l_e were extracted from a fit to $\overline{\mathcal{T}} = N/(1 + L/l_e)$ throughout the range of lengths $0 < L < L_0$ where $\overline{\mathcal{T}}$ provides a better statistical description of the transmission than $\ln\overline{\mathcal{T}}$ (i.e., L such that $\Delta\mathcal{T}/\overline{\mathcal{T}} < \Delta\ln\mathcal{T}/\ln\overline{\mathcal{T}}$, $\Delta\mathcal{T} = (\overline{\mathcal{T}^2} - \overline{\mathcal{T}}^2)^{1/2}$) [16]. On the other hand, the localization lengths ξ were interpolated from $\ln\overline{\mathcal{T}} = -L/\xi$ for $L > L_0$. In addition to the approximate $\sim\omega^{-2}$ behavior, in accordance with the Rayleigh formula for 1D systems, both length scales display signatures of the underlying phonon band structure: drops close to the band edges due to the reduced group velocity and transmission probability.

The localization length is commonly related to the mean free path via the Thouless relation $\xi \sim Nl_e$ [22,23]. Under assumptions of weak disorder and isotropic scattering in quasi-1D systems where diffusive ($l_e \ll L \ll \xi$) and localized regimes ($L \gg \xi$) are clearly separable, this relation was shown to be independent of the type of disorder and the band structure [24]. However, the separation of transport regimes in our particular system is not so clear-cut because of a relatively small number of transport channels ($N \sim 10$); therefore, it is not *a priori* apparent if the Thouless relation should hold. The Fig. 2 inset compares the ratio ξ/l_e with the predictions of the Thouless relation in the whole frequency spectrum. The agreement is quite good (similarly as for electrons in NTs [16] and NWs [17]), except for lower ω (where ξ cannot be calculated properly because they become similar to the maximal L considered) and $\omega \approx 230$ THz (where l_e could not be extracted accurately due to strong backscattering even for short L).

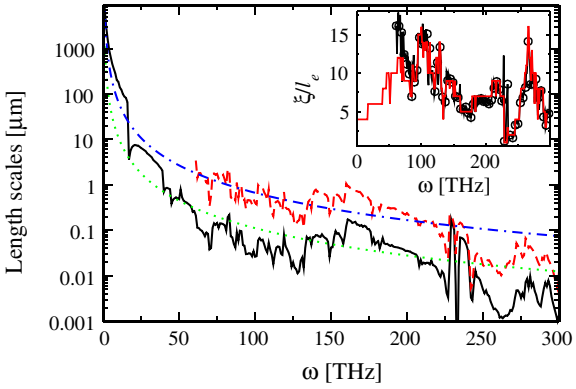

FIG. 2 (color online). Transport length scales versus frequency dependence for (7, 0) carbon nanotubes with 10.7% of ^{14}C isotopes. Solid black and dashed red lines represent the mean free paths and localization lengths, respectively. Dash-dotted blue and dotted green lines correspond to estimated relaxation lengths for temperatures of 50 and 300 K, respectively. Inset: the localization length over the mean free path ratio as a function of frequency (solid black line with circles), compared with the number of phonon bands of the perfect nanotube (solid red line).

The transition to the localized regime for a certain phonon frequency will happen only if incoherent effects are weak enough so that phonons preserve their phase coherence up to the localization length. In the opposite case, the conduction is determined by the interplay between coherent multiple scattering and incoherent effects. The inclusion of both phenomena on an equal footing into the present Green's function formalism for long nanotubes is an extremely challenging problem and merits a separate study. Nonetheless, localization and anharmonic relaxation lengths can be directly confronted in order to know whether localization will take place.

A rough estimate of the order of magnitude of the anharmonic relaxation length in graphite materials has been given as $l_\phi = BT^{-1}\omega^{-2}$, $B = 3.35 \times 10^{23}$ m K s^{-2} [25]. Despite its very crude character, this approximation is able to correctly describe the transition from ballistic to diffusive phonon transport in defect free CNTs [26]. The relaxation lengths for the temperatures of 50 and 300 K are shown by dash-dotted and dotted lines, along with the mean free paths and localization lengths, in Fig. 2. Even for T as low as 50 K, ξ and l_ϕ are comparable for most frequencies. Hence, it is likely that, for the considered concentration of isotopes, localization effects will not take place. On the other hand, for T lower than 50 K and L up to a few μm, only low frequency quasiballistic phonons contribute to the thermal conduction.

But even if localization were not destroyed by anharmonic scattering, it would still not be observable by direct thermal conductivity measurements. This is because a large proportion of quasiballistic low frequency phonons coexists with the diffusive and localized higher frequency phonons. The thermal conductance value is dominated by the much larger ballistic and diffusive contributions. Thus, if the localized phonons behaved diffusive instead [$\overline{\mathcal{T}} = N/(1 + L/l_e)$ for all L], the difference in thermal conductance would be negligible, as shown in Fig. 3. In contrast, localization effects in the case of electrons are manifested via an exponential decrease of the conductance with the nanotube length even at the room temperature [21,27], due to almost simultaneous localization of all electrons from the energy range of $\sim k_B T$ around the Fermi energy [16,27], where k_B is the Boltzmann constant.

Let us now consider the diffusive regime, taking place at lengths intermediate between the ballistic and localized ones. It is often assumed that, in the diffusive regime for low disorder concentrations, WI effects due to multiple scattering cancel out as a result of random phases of different scattering paths. In such case, it can be shown [15] that the total transmission in the presence of N_i impurities is $1/\mathcal{T} = N_i/\mathcal{T}_1 - (N_i - 1)/\mathcal{T}_0$, where $\mathcal{T}_1$ is the one impurity transmission, and $\mathcal{T}_0$ is the transmission of the impurity free system. To see how much this "incoherent" approximation differs from the exact calculation, in Fig. 4 we show the mean free paths extracted from the full calculation and this approximate approach, as a function of frequency (solid and dashed lines, respectively). There is a quite good agreement for low disorder concentrations (also observed for electrons in NTs [28] and NWs [17]). Thus, for concentrations $<1\%$, the mean free paths and, hence, the thermal conductivity can be fairly well estimated from the approximate approach, as well as the localization lengths using the Thouless relation.

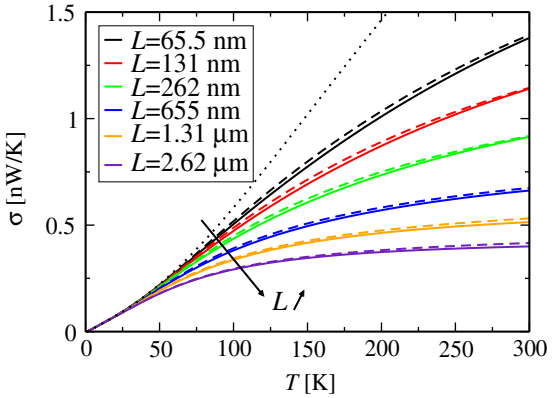

FIG. 3 (color online). Thermal conductance as a function of temperature for (7, 0) carbon nanotubes with 10.7% of ^{14}C isotopes for several lengths. The solid and dashed lines represent the exact calculation and an approximate one which neglects localization effects, respectively. The dotted line corresponds to the perfect nanotube case.

On the other hand, for large isotope concentrations ($\gtrsim$10%), multiple scattering driven WI effects lead to actual mean free paths which may differ from the "incoherent" approximation results by a factor of 2 or larger (see Fig. 4). The effect of such high isotope concentrations on thermal conductance has been experimentally reported for natural-abundance BN multiwalled NTs (MWNTs) (19.9% of ^{10}B and 80.1% of ^{11}B) [2]. Since the contact resistance was found to be minimal in small diameter ($\approx$1 nm) single-walled NTs (SWNTs) [29], the ratio of measured thermal conductivity κ between isotope pure and impure SWNTs should be independent of this effect. Our results

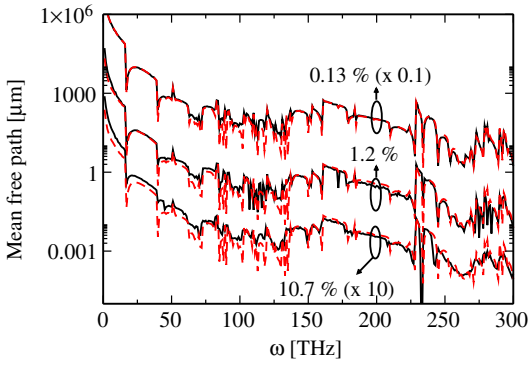

FIG. 4 (color online). Mean free paths versus frequency for (7, 0) carbon nanotubes with several concentrations of ^{14}C isotopes. The scaling factors are given in brackets. Solid lines represent the exact calculation, while dashed ones correspond to an approximate calculation which neglects interference.

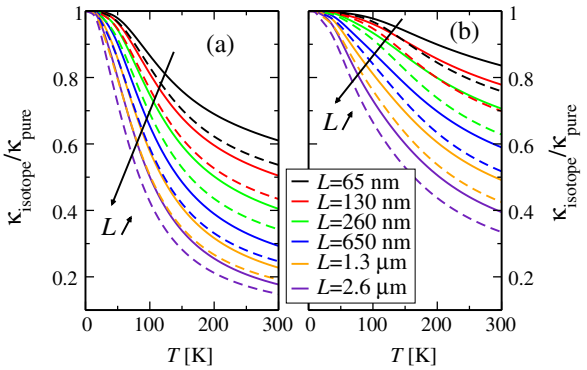

FIG. 5 (color online). The ratio of the thermal conductivities for disordered and perfect nanotubes versus temperature dependence for several lengths of (a) (7, 0) carbon nanotubes with 10.7% of ^{14}C isotopes, and (b) (8, 0) boron-nitride nanotubes with 18.8% of ^{10}B isotopes. Solid and dashed lines correspond to the exact calculation and an approximate one which neglects interference effects, respectively.

yield concrete predictions for the ratio $\kappa_{\text{isotope}}(T)/\kappa_{\text{pure}}(T)$ for different NT lengths. They are given by solid lines in Figs. 5(a) and 5(b), for (7, 0) CNT with 10.7% of ^{14}C isotopes and (8, 0) BN NT with 18.8% of ^{10}B, respectively. In the same figure we show in dashed lines that, if WI effects due to multiple scattering could be neglected, this ratio for a certain length would be similar to the accurate result for roughly 2 times longer lengths. Thus, multiple scattering induced WI effects play an important role in limiting the reduction of the thermal conductivities in high concentration isotope-disordered C and BN NTs.

We should note that the ratio $\kappa_{\text{isotope}}(T)/\kappa_{\text{pure}}(T)$ for SWNTs is no longer expected to match our harmonic calculation for L larger than a few μm above room temperature, since anharmonic scattering becomes important [29,30]. The predicted isotope effect reduction of the BN SWNTs thermal conductance is very strong, comparable to those experimentally reported for MWNTs ($\approx$0.5). It takes place despite the fact that no localization effects will be observable, contrary to prior speculations. The calculated results may be directly compared against measurements on single-walled samples with controlled isotope concentration, should the latter become available in the future.

In conclusion, we have answered a controversial question on the origin of observable reductions of the thermal conductivity in isotope-disordered C and BN NTs. This effect was shown to be a consequence of diffusive scattering, and not of localization effects, as it was previously argued. Interference phenomena due to multiple scattering were found to be important for the thermal conduction properties of high isotope concentration ($\gtrsim$10%) samples. For smaller concentrations, we demonstrated that the phonon conduction is well described by the additive contributions of single scatterers. The concrete magnitude of the predicted isotope effects could be tested by future thermal conductivity measurements on single-walled nanotubes.

This project was supported in part by an IRG grant from the EU, and by NSF Grants No. 0651310 and No. 0651427. We acknowledge precious discussions with R. Avriller, B. Biel, S. Roche, L. Lindsay, and D. A. Broido.

[1] D. G. Cahill, W. K. Ford, K. E. Goodson, G. D. Mahan, A. Majumdar, H. J. Maris, R. Merlin, and S. R. Phillpot, J. Appl. Phys. **93**, 793 (2003).
[2] C. W. Chang, A. M. Fennimore, A. Afanasiev, D. Okawa, T. Ikuno, H. Garcia, D. Li, A. Majumdar, and A. Zettl, Phys. Rev. Lett. **97**, 085901 (2006).
[3] M. P. Blencowe, J. Phys. Condens. Matter **7**, 5177 (1995).
[4] A. Kambili, G. Fagas, V. I. Falko, and C. J. Lambert, Phys. Rev. B **60**, 15 593 (1999).
[5] B. A. Glavin, Phys. Rev. Lett. **86**, 4318 (2001).
[6] D. H. Santamore and M. C. Cross, Phys. Rev. Lett. **87**, 115502 (2001).
[7] P. G. Murphy and J. E. Moore, Phys. Rev. B **76**, 155313 (2007).
[8] C. Chiritescu, D. G. Cahill, N. Nguyen, D. Johnson, A. Bodapati, P. Keblinski, and P. Zschack, Science **315**, 351 (2007).
[9] N. Yang, G. Zhang, and B. Li, Nano Lett. **8**, 276 (2008).
[10] J. Che, T. Çağin, and W. A. Goddard III, Nanotechnology **11**, 65 (2000).
[11] T. Yamamoto and K. Watanabe, Phys. Rev. Lett. **96**, 255503 (2006).
[12] N. Mingo, D. A. Stewart, D. A. Broido, and D. Srivastava, Phys. Rev. B **77**, 033418 (2008).
[13] G. Zhang and B. Li, J. Chem. Phys. **123**, 114714 (2005).
[14] J. Shiomi and S. Maruyama, Phys. Rev. B **74**, 155401 (2006).
[15] S. Datta, *Electronic Transport in Mesoscopic Systems* (Cambridge University Press, Cambridge, U.K., 1995).
[16] R. Avriller, S. Latil, F. Triozon, X. Blase, and S. Roche, Phys. Rev. B **74**, 121406(R) (2006).
[17] T. Markussen, R. Rurali, A.-P. Jauho, and M. Brandbyge, Phys. Rev. Lett. **99**, 076803 (2007).
[18] N. Mingo and L. Yang, Phys. Rev. B **68**, 245406 (2003).
[19] J. M. Soler, E. Artacho, J. D. Gale, A. García, J. Junquera, P. Ordejón, and D. Sánchez-Portal, J. Phys. Condens. Matter **14**, 2745 (2002).
[20] D. A. Stewart *et al.* (to be published).
[21] C. Gomez-Navarro, P. J. D. Pablo, J. Gomez-Herrero, B. Biel, F. J. Garcia-Vidal, A. Rubio, and F. Flores, Nature Mater. **4** (2005).
[22] D. J. Thouless, Phys. Rev. Lett. **39**, 1167 (1977).
[23] P. W. Anderson, D. J. Thouless, E. Abrahams, and D. S. Fisher, Phys. Rev. B **22**, 3519 (1980).
[24] C. W. J. Beenakker, Rev. Mod. Phys. **69**, 731 (1997).
[25] P. G. Klemens and D. F. Pedraza, Carbon **32**, 735 (1994).
[26] N. Mingo and D. Broido, Nano Lett. **5**, 1221 (2005).
[27] B. Biel, F. J. Garcia-Vidal, A. Rubio, and F. Flores, Phys. Rev. Lett. **95**, 266801 (2005).
[28] T. Kostyrko, M. Bartkowiak, and G. D. Mahan, Phys. Rev. B **60**, 10 735 (1999).
[29] C. Yu, L. Shi, Z. Yao, D. Li, and A. Majumdar, Nano Lett. **5**, 1842 (2005).
[30] E. Pop, D. Mann, Q. Wang, K. Goodson, and H. Dai, Nano Lett. **6**, 96 (2006).